

- [1] a) D. Zhang, L. Qi, J. Ma, H. Cheng, *Adv. Mater.* **2002**, *14*, 1499. b) Z. Yang, Z. Niu, Y. Lu, Z. Hu, C. C. Han, *Angew. Chem. Int. Ed.* **2003**, *42*, 1943.
- [2] a) C. Niemeyer, *Angew. Chem. Int. Ed.* **2001**, *40*, 128. b) C. R. Vestal, Z. J. Zhang, *J. Am. Chem. Soc.* **2002**, *124*, 14312. c) P. Tartaj, C. J. Serna, *J. Am. Chem. Soc.* **2003**, *125*, 15754.
- [3] a) B. Martínez, X. Obradors, L. I. Balcells, A. Rovagnet, C. Monty, *Phys. Rev. Lett.* **1998**, *80*, 181. b) P. Tartaj, T. González-Carreño, C. J. Serna, *J. Phys. Chem. B* **2003**, *107*, 20. c) S. Sun, S. Anders, T. Thomson, J. E. E. Baglin, M. F. Toney, H. F. Hamann, C. B. Murray, B. D. Terris, *J. Phys. Chem. B* **2003**, *107*, 5419. d) F. X. Redl, K.-S. Cho, C. B. Murray, S. O. O'Brien, *Nature* **2003**, *423*, 968.
- [4] P. Allia, M. Coisson, P. Tiberto, F. Viani, M. Knobel, M. A. Novak, W. C. Nunes, *Phys. Rev. B: Condens. Matter Mater. Phys.* **2001**, *64*, 144420.
- [5] P. Tartaj, M. P. Morales, S. Veintemillas-Verdaguer, T. Gonzalez-Carreño, C. J. Serna, *J. Phys. D: Appl. Phys.* **2003**, *36*, R182.
- [6] Q. A. Pankhurst, J. Connolly, S. K. Jones, J. Dobson, *J. Phys. D: Appl. Phys.* **2003**, *36*, R167.
- [7] a) M. Zhao, L. Josephson, Y. Tang, R. Weissleder, *Angew. Chem. Int. Ed.* **2003**, *42*, 1375. b) A. Dyal, K. Loos, M. Noto, S. W. Chang, C. Spagnoli, K. V. P. M. Shafi, A. Ulman, M. Cowman, R. A. Gross, *J. Am. Chem. Soc.* **2003**, *125*, 1684. c) Y. Weizmann, F. Patolovsky, E. Katz, I. Willner, *J. Am. Chem. Soc.* **2003**, *125*, 3452.
- [8] B. Xia, I. W. Lenggoro, K. Okuyama, *Adv. Mater.* **2001**, *13*, 1579.
- [9] P. Tartaj, T. González-Carreño, C. J. Serna, *Langmuir* **2002**, *18*, 4556.
- [10] P. Tartaj, T. González-Carreño, C. J. Serna, *Adv. Mater.* **2001**, *13*, 1620.
- [11] B. Martinez, A. Roig, E. Molins, T. González-Carreño, C. J. Serna, *J. Appl. Phys.* **1998**, *83*, 3256.
- [12] Evidence of hollowness in the samples was corroborated by scanning electron microscopy. Using this technique we observed a similar microstructure in all samples. In the scanning mode we only observed the surface of particles, and since the resolution is much smaller than in the transmission mode, we can expect dense and hollow spheres to appear similar.
- [13] M. El-Hilo, K. O'Grady, R. W. Chantrell, *J. Magn. Magn. Mater.* **1992**, *114*, 295.
- [14] S. Mørup, F. Bødker, P. V. Hendriksen, S. Linderth, *Phys. Rev. B: Condens. Matter Mater. Phys.* **1995**, *52*, 287.
- [15] C. Binns, M. J. Maher, Q. A. Pankhurst, D. Kechrakos, K. N. Trohidou, *Phys. Rev. B: Condens. Matter Mater. Phys.* **2002**, *66*, 184413.
- [16] C. Kittel, *Introduction to Solid State Physics*, Wiley, New York **1968**.
- [17] K. O'Grady, A. Bradbury, *J. Magn. Magn. Mater.* **1983**, *39*, 91.
- [18] P. Tartaj, *ChemPhysChem* **2003**, *4*, 1371.
- [19] According to Equation 2 the parameter T^* depends not only on α and N but also on M_S . Because M_S depends on temperature we can expect differences in the value of T^* at different temperatures. This is the reason why we estimate T^* at 300 K (working temperature for most of the relevant technological applications of magnetic nanoparticles).
- [20] A fit with Equation 3, superimposed with a log-normal particle size distribution results in strongly correlated parameters of T^* and the median particle size. However, the agreement between the particle size estimated following this model and that estimated from X-ray diffraction seems to suggest that the fit was reliable. In any case, it is clear that the mean field model is successful in describing dipolar interactions between nanomagnets.
- [21] A. A. Kuznetsov, V. I. Filippov, R. N. Alyautdin, N. L. Torshina, O. A. Kuznetsov, *J. Magn. Magn. Mater.* **2001**, *225*, 95.
- [22] A. Voigt, N. Buske, G. B. Sukhorukov, A. A. Antipov, S. Leporatti, H. Lichtenfeld, H. Bäumlner, E. Donath, H. Möhwald, *J. Magn. Magn. Mater.* **2001**, *225*, 59.

Enhancement in the Orientation of the Microdomain in Block Copolymer Thin Films upon the Addition of Homopolymer**

By *Unyong Jeong, Du Yeol Ryu, Dong Han Kho, Jin Kon Kim,* James T. Goldbach, Dong Ha Kim, and Thomas P. Russell**

Thin films of block copolymers with well-defined nanoscale structures have recently gained much attention for their potential uses as functional nanostructures.^[1-7] Thin films with cylindrical microdomains can be used as etching masks for pattern transfer to a substrate^[6] and as scaffolds for the fabrication of arrays of nanowires.^[3] Such arrays can be used in magnetic storage,^[4] as isolation sites for nanocrystals to increase optical properties,^[7] or as field-emission devices. For addressable media, both the orientation and long-range lateral ordering of the cylindrical microdomains in thin films are essential. In thin films, balancing interfacial interactions causes a directed self-assembly of microdomains normal to the substrate surface when the thin film thickness (h) is one lattice spacing (L_0) or less.^[8-12] This limits the aspect ratio (h/L_0) of the cylindrical microdomains to ~ 2 . To overcome this length limitation, external fields can be used to orient the microdomains in films of arbitrary thickness.^[3,4] Alternatively, solvent field,^[13-15] patterned surfaces,^[16-18] confinement,^[19,20] and surface topography^[21,22] can be used to similar ends.

Even though theory^[23,24] and simulations^[25-27] suggest that it should be possible to maintain the orientation of cylindrical microdomains normal to the surface in thick films, it has not yet been realized experimentally. Here, the addition of poly(methyl methacrylate) (PMMA) homopolymer to an asymmetric polystyrene-*block*-poly(methyl methacrylate) copolymer (PS-*b*-PMMA) is shown to produce a drastic increase in the persistence of the orientation of nanodomains normal to the surface, enabling a directed self-assembly of the copoly-

[*] Prof. J. K. Kim, Dr. U. Jeong, Dr. D. Y. Ryu, D. H. Kho
Department of Chemical Engineering and Polymer Research Institute
Electronic and Computer Engineering Divisions
Pohang University of Science and Technology
Kyungbuk 790-784 (Korea)
E-mail: jkkim@postech.ac.kr

Prof. T. P. Russell, J. T. Goldbach, D. H. Kim
Silvio O. Conte National Center for Polymer Research
Department of Polymer Science and Engineering
University of Massachusetts at Amherst
Amherst, MA 01003 (USA)
E-mail: Russell@mail.pse.umass.edu

[**] This work was supported by the National R & D project for Nano Science and Technology (M1-0214-00-0230), the Department of Energy, Office of Basic Energy Sciences under contract DE-FG02-96ER45612, National Science Foundation under partnership in Nanotechnology (CTR-9871782), and the Material Research Science and Engineering Center at the University of Massachusetts. Small angle X-ray scattering was performed at PLS beam line supported by POSCO and KOSEF.

mers into arrays of highly oriented, high-aspect-ratio cylindrical microdomains over large areas.

Figure 1 shows scanning electron microscopy (SEM) images of thin films of two different PS-*b*-PMMA. One (AP-88) with weight-average molecular weight (M_w) of 88 000 was prepared by anionic polymerization (AP) and annealed at 165 °C for

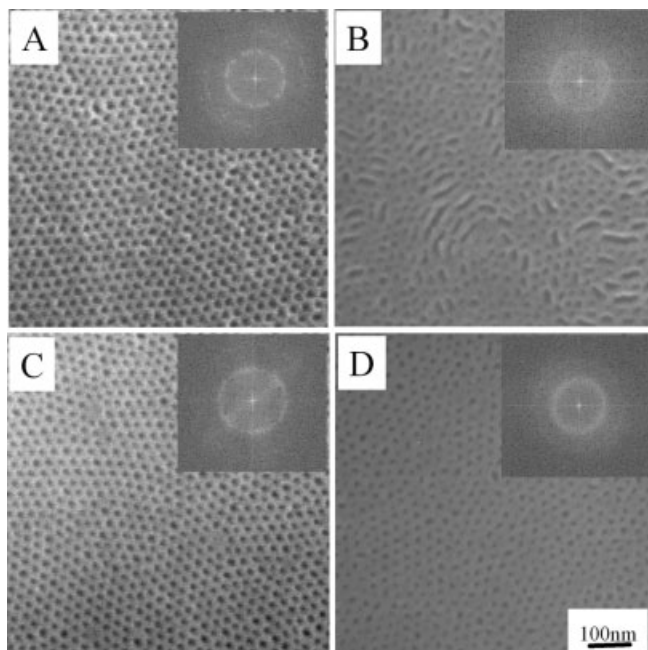


Figure 1. SEM micrographs of AP-88 (A,B) and ATRP-71 (C,D) with different h values. A) 34 nm. B) 43 nm. C) 61 nm. D) 74 nm. AP-88 was annealed at 165 °C for 2 days, whereas ATRP-71 was annealed at 150 °C for 2 days. All PMMA phases were etched using UV.

two days, and the other (ATRP-71) with M_w of 71 000 was prepared by atom-transfer radical polymerization (ATRP) and annealed at 150 °C for two days. Thin films of AP-88 and ATRP-71 were also annealed at various temperatures between 130 °C and 180 °C. The best perpendicular orientation of the cylindrical microdomains for AP-88 was obtained when the film was annealed at 160–170 °C. If the film was annealed at temperatures higher than 180 °C, a mixed morphology of perpendicular and parallel orientations was observed. However, when annealed below 150 °C, the film showed poor hexagonal packing of the microdomains. The best perpendicular orientation of neat ATRP-71 was found when the film was annealed at 145–165 °C, although a good perpendicular orientation was observed even when annealed at 140 °C and 180 °C. As shown in Figures 1A,B, an array of cylindrical microdomains oriented normal to the surface was obtained for a 34 nm thick film ($h/L_o \approx 1$) of AP-88, whereas a mixed morphology consisting of cylinders oriented parallel and perpendicular to the surface was obtained when $h=43$ nm. In the case of ATRP-71, even though the morphology is the same, much thicker films are seen to produce cylinders normal to the surface, as shown in Figure 1C for a 61 nm thick film. However, increasing the film thickness causes the orientation

of the microdomains to deteriorate (cf. the results for a 74 nm thick film shown in Fig. 1D).

To explain the difference in the degree of perpendicular orientation between AP-88 and ATRP-71, two homopolymers of PMMA (PMMA-AP and PMMA-ATRP) were synthesized by AP and ATRP methods. We found that the surface tensions of the two PMMA homopolymers are the same. Furthermore, the interfacial tension between PS and PMMA, as well as that between a random PS-PMMA copolymer (PS-*ran*-PMMA) and PMMA, did not change for the two PMMA homopolymers. We consider that the main reason for this is the different chain mobility related to the T_g of the PMMA blocks. We found that PMMA-AP shows a higher syndiotacticity ($mm=0.01$, $mr=0.20$, $rr=0.79$), measured by ^1H NMR spectroscopy, whereas PMMA-ATRP shows a smaller syndiotacticity ($mm=0.06$, $mr=0.37$, $rr=0.56$). The T_g of PMMA-AP, measured by differential scanning calorimetry (Perkin-Elmer DSC-7 series) at a heating rate of 10 °C/min, is 134 °C, which is 30 °C higher than that of PMMA-ATRP. On the other hand, the tacticity and the T_g of PS prepared by AP are essentially the same as those prepared by ATRP.

Figures 2A–C show SEM images of films of ATRP-71/PMMA-18 (where 18 denotes that the M_w of the homopolymer is 18 000) mixtures where the thicknesses of the films were 90 nm, 278 nm, and 329 nm, respectively. The volume fraction (ϕ_H) of PMMA-18 based on the total amount of PMMA (the sum of PMMA in the homopolymer and copolymer) was 0.26. The film mixtures were annealed at 150 °C for two days. Field-emission SEM (FE-SEM) images show a hexagonal packing of the cylindrical microdomains at the surface

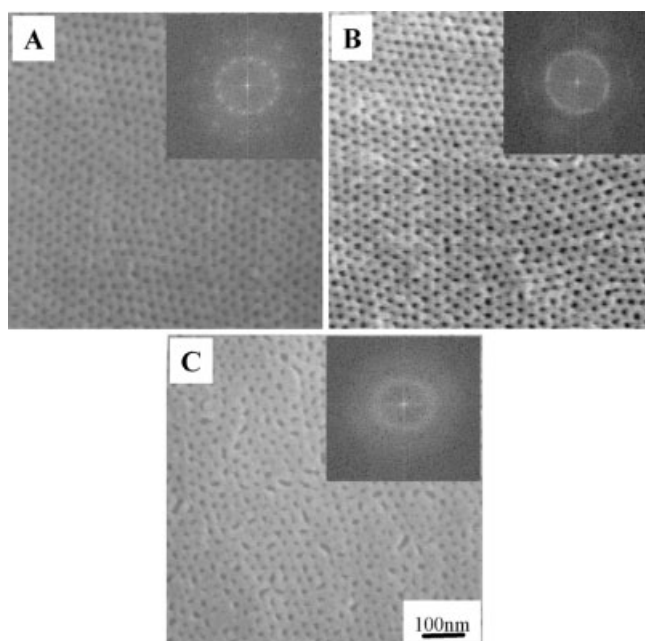


Figure 2. SEM micrographs of thin film mixtures of ATRP-71/PMMA-18 at fixed ϕ_H (0.26) for three different values of h . A) 91 nm. B) 278 nm. C) 329 nm. All samples were annealed at 150 °C for 2 days. All PMMA phases were etched using UV.

of the film, even for a 300 nm thick film (approx. $10 L_o$). For films thicker than about 310 nm, the hexagonal packing at the surface starts to decrease, as shown in Figure 2C. However, the observation of the hexagonal packing of microdomains at the air surface does not prove that cylindrical microdomains span the entire thickness of the film. The FE-SEM images of the fracture surfaces of 92 nm and 273 nm thick films (Figs. 3A and 3B, respectively) show both the film surface and a cross-section. The top surfaces show arrays of hexagonally packed cylindrical nanopores, whereas the cross-section demonstrates that these nanopores are oriented normal to the sub-

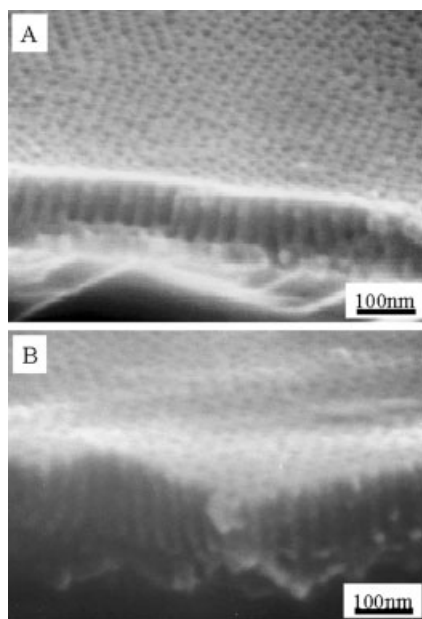


Figure 3. Cross-sectional SEM images for mixtures of ARR-71/PMMA-18 with ϕ_H of 0.26 at two different film thicknesses: A) 92 nm and B) 329 nm. All PMMA phases were etched using UV.

strate and penetrate through the entire film. It is evident that the added homopolymer plays a key role in guiding the assembly of block copolymers.

The distribution of the homopolymer in the cylindrical microdomain depends strongly on the amount (ϕ_H) of added homopolymer, the ratio of the molecular weight of PMMA homopolymer to PMMA block (α), and the interactions between the homopolymer and both blocks of the copolymer.^[28–30] Previously, it was shown that PMMA homopolymer chains in a PS-*b*-PMMA/PMMA mixture with $\alpha = 0.24$ were uniformly distributed within the cylindrical microdomains. By increasing the molecular weight of the homopolymer, such that $\alpha = 1.76$, the homopolymer was found to be highly localized at the center of PMMA cylindrical microdomains.^[28] At a fixed ϕ_H (0.26), the maximum thickness (h_{\max}) where a normal orientation of cylindrical microdomains was maintained increased with increasing α . If, on the other hand, the molecular weight of the homopolymer was fixed, and equal to that of the block ($\alpha = 1.0$), then as ϕ_H increased from 0.15 to 0.33, h_{\max} increased from about

110 nm to about 340 nm. It should be noted that even for $\phi_H = 0.33$, the cylindrical microdomain morphology remained, with no transition to a lamellar microdomain morphology. However, for $\phi_H \approx 0.4$, a macrophase separation occurred in the thin films.^[28] Finally, when a PMMA homopolymer with $\alpha = 0.24$ was used, we could not observe any discernible increase in h_{\max} (less than $\pm 10\%$) compared with that of neat block copolymer, even when ϕ_H was increased to 0.33.

From the results discussed above it is clear that the extent to which the homopolymer is localized within the cylindrical microdomains can influence the assembly of the copolymers in the thin films and the range over which order and orientation will propagate from the surface. This results from the conformation that the homopolymer must assume within the confined volume of the cylindrical microdomain in comparison to that of the minor component block of the copolymer. As the confinement of the homopolymer to the center of the cylindrical microdomain increases, the homopolymer is forced to adopt a conformation that is stretched along the cylinder axis, as confirmed by a simulation, which shows that the difference between $R_{g,z}^2$ and $(R_{g,x}^2 + R_{g,y}^2)/2$ increases with increasing molecular weight (or increasing confinement of the homopolymer).^[31] Here, $R_{g,z}^2$ is the mean square radius of gyration of the homopolymer in the z -direction (cylinder axis direction), while $R_{g,x}^2$ and $R_{g,y}^2$ are those in the x - and y -directions, respectively. Thus, as the self-assembly and orientation of the cylindrical microdomains occurs in the thin films, the homopolymer chains are incorporated within each cylindrical microdomain and extend or protrude along the cylinder axis. As the oriented microdomains propagate into the interior of the film, the embedded homopolymer guides subsequent assembly. Consequently, the directionality of the ordering is significantly enhanced by the presence of the homopolymer. The degree to which this occurs depends, of course, on the degree of confinement of the homopolymer chains. If the molecular weight of the homopolymer is roughly less than one-half that of the copolymer block ($\alpha < 0.5$), the homopolymer is uniformly dispersed in the cylinder^[28] and no enhancement is seen. If, on the other hand, $\alpha > 3$, the homopolymer is excluded from the microdomain, macrophase separation occurs,^[28] and no enhancement in the orientation is seen. However, for $0.5 < \alpha < 3$, the homopolymer is incorporated into the copolymer, and with increasing α , the confinement increases and an enhancement in the order and orientation is observed. At α values of about 1.5, a maximum enhancement in the orientation of the microdomains is seen. With increasing molecular weight of the homopolymer, the confinement and consequent deformation of the homopolymer chain along the axis of the cylindrical microdomain increases. However, the possibility for macrophase separation of the homopolymer from the microdomain also increases. Thus, this balance between chain deformation and solubility gives rise to a specific molecular weight where maximal enhancement is observed.

The simple addition of homopolymer can therefore be used to markedly promote microdomain orientation without the use of external fields. Large degrees of localization (large val-

ues of α) without phase transition can enhance vertical orientation (thus, larger h_{\max}) with increasing ϕ_H . This streamlines the process for producing arrays of very high aspect ratio nanostructures in thin films, which is significant for the application of these materials in fabrication processes. In combination with our previous work,^[32–34] very high aspect ratio nanopores with various diameters can also be fabricated.

Experimental

PS-*b*-PMMA (ATRP-71) was prepared by an atom-transfer radical polymerization technique. The PMMA block was initially synthesized using ethyl 2-bromoisobutyrate as an initiator and a mixture of copper(I) bromide (CuBr) and 4,4'-dinonyl-2,2'-bipyridine (dNbpy) as a catalyst in a 50 % solution of MMA monomer in benzene [35,36]. This polymer was precipitated in about 1 L of hexane, filtered and dried. It was then re-dissolved in about 100 mL of tetrahydrofuran (THF) and passed through a column of silica gel (8 × 40 cm) with THF as eluent. The purified polymer was precipitated in excess hexanes, and dried in vacuo. The weight average molecular weight (M_w) and polydispersity index (M_w/M_n) were 19 000 and 1.10, respectively, as measured by gel permeation chromatography (Waters Co.) using PMMA standards. A 3.0 g sample of the purified, dry PMMA obtained from the previous step was then added to a nitrogen-purged Schlenk flask, evacuated and back-filled with nitrogen. The mixture of CuBr and dNbpy (five equivalents per PMMA end group) was then added. Distilled styrene (10.0 mL) and distilled benzene (10.0 mL) were then added from a syringe, and the mixture was stirred at 75 °C for 6 h. Upon cooling, the block copolymer was precipitated in excess methanol three times, filtered and dried in vacuo. All the dead PMMA and PS homopolymers in the PS-*b*-PMMA were completely removed by acetic acid and cyclohexane extractions respectively, which were monitored by GPC and ¹H NMR spectroscopy. The volume fraction of PMMA block of ATRP-71 was 0.27, and the M_w and the polydispersity index were 71 000, and 1.09, respectively.

To compare the effect of the tacticity of the PMMA block on the cylindrical microdomain orientation, another PS-*b*-PMMA (AP-88) was synthesized anionically by sequential addition of styrene and methyl methacrylate (MMA) with an initiator of *sec*-butyllithium (*s*-BuLi) in THF at –78 °C under a purified argon atmosphere, with an additional five equivalents of lithium chloride (LiCl) relative to *s*-BuLi [28]. The block copolymer anion was terminated by addition of degassed methanol. The volume fraction of PMMA block in AP-88 was 0.27, and the M_w and polydispersity index were 88 000, and 1.04, respectively. A benzyl-alcohol-terminated random copolymer of styrene and MMA, denoted PS-*ran*-PMMA, with a styrene mole fraction of 0.58, weight average molecular weight (M_w) of 11,000, and polydispersity index of 1.13, was used to prepare energetically neutral surfaces [11]. The PMMA homopolymer (PMMA-18) with M_w and polydispersity index of 18 000 and 1.05, respectively, was synthesized anionically.

Thin films of PS-*b*-PMMA and mixtures with PMMA homopolymer were prepared by spin-coating toluene solutions onto silicon substrates modified with the random copolymer brush. The film thickness was varied from about 25 nm to about 500 nm by adjusting the solution concentration and spin speed. Thin films were annealed at elevated temperatures under vacuum, and then quenched to room temperature.

The lattice spacing of the cylindrical microdomains (L_o) of 1.5 mm thick PS-*b*-PMMA samples was measured by small-angle X-ray scattering (SAXS) on beam line 4C1 at the Pohang Light Source (PLS), Korea [37]. The surface morphology was studied by field-emission scanning electron microscopy (FE-SEM, Hitachi S-4200) after ultraviolet etching followed by acetic acid washing. Cross-sectional images of the cylindrical microdomains in the films were obtained by FE-SEM after cutting the silicone substrate at room temperature.

Received: September 4, 2003
Final version: December 18, 2003

- [1] M. Park, C. K. Harrison, M. Chaikin, R. A. Register, D. H. Adamson, *Science* **1997**, *276*, 1407.
- [2] A. Averopoulos, V. Z.-H. Chan, V. Y. Lee, D. No, R. D. Miller, N. Hadjichristidis, N. L. Thomas, *Chem. Mater.* **1998**, *10*, 2109.
- [3] T. Thurn-Albrecht, J. Schotter, A. Kästle, N. Emley, T. Shibauchi, L. Krusin-Elbaum, K. Guarini, C. T. Black, M. T. Tuominen, T. P. Russell, *Science* **2000**, *290*, 2126.
- [4] T. Thurn-Albrecht, R. Steiner, J. DeRouchey, C. M. Stafford, E. Huang, M. Ball, M. T. Tuominen, C. J. Hawker, T. P. Russell, *Adv. Mater.* **2000**, *12*, 787.
- [5] C. T. Black, K. W. Guarini, K. R. Milkove, S. M. Baker, M. T. Tuominen, T. P. Russell, *Appl. Phys. Lett.* **2001**, *79*, 409.
- [6] P. Mansky, C. K. Harrison, P. M. Chaikin, R. A. Register, N. Yao, *Appl. Phys. Lett.* **1996**, *68*, 2586.
- [7] M. J. Misner, H. Skaff, T. Emrick, T. P. Russell, *Adv. Mater.* **2003**, *15*, 221.
- [8] M. S. Turner, *Phys. Rev. Lett.* **1992**, *69*, 1788.
- [9] P. Lambooy, T. P. Russell, G. J. Kellogg, *Phys. Rev. Lett.* **1994**, *72*, 2899.
- [10] G. J. Kellogg, D. G. Walton, A. M. Mayes, P. Lambooy, T. P. Russell, *Phys. Rev. Lett.* **1996**, *76*, 2503.
- [11] P. Mansky, Y. Liu, E. Huang, T. P. Russell, C. J. Hawker, *Science* **1997**, *275*, 1458.
- [12] E. Huang, L. Rockford, T. P. Russell, C. J. Hawker, J. Mays, *Nature* **1998**, *395*, 757.
- [13] G. Kim, M. Libera, *Macromolecules* **1998**, *31*, 2569.
- [14] G. Kim, M. Libera, *Macromolecules* **1998**, *31*, 2670.
- [15] S. H. Kim, M. J. Misner, T. Xu, M. Kimura, T. P. Russell, *Adv. Mater.* **2004**, *16*, 226.
- [16] L. Rockford, Y. Liu, P. Mansky, T. P. Russell, M. Yoon, S. G. Mochrie, *Phys. Rev. Lett.* **1999**, *82*, 2602.
- [17] L. Rockford, S. G. Mochrie, T. P. Russell, *Macromolecules* **2000**, *34*, 1487.
- [18] S. O. Kim, H. H. Solak, H. Stoykovich, N. J. Ferrie, J. J. de Pablo, P. F. Nealey, *Nature* **2003**, *424*, 411.
- [19] G. T. Pickett, A. C. Balazs, *Macromolecules* **1997**, *30*, 3097.
- [20] M. S. Turner, J. F. Joanny, *Macromolecules* **1992**, *25*, 6681.
- [21] M. J. Fasolka, D. H. Harris, A. M. Mayes, M. Yoon, S. J. Mochrie, *Phys. Rev. Lett.* **1997**, *79*, 3018.
- [22] E. Sivaniah, Y. Hayashi, M. Iino, T. Hahimoto, K. Fukunaga, *Macromolecules* **2003**, *36*, 5894.
- [23] G. Brown, A. Chakrabarti, *J. Chem. Phys.* **1995**, *102*, 1440.
- [24] K. Y. Suh, Y. S. Kim, H. H. Lee, *J. Chem. Phys.* **1998**, *108*, 1253.
- [25] Q. Wang, P. F. Nealey, J. J. de Pablo, *Macromolecules* **2003**, *36*, 1731.
- [26] Q. Wang, P. F. Nealey, J. J. de Pablo, *Macromolecules* **2001**, *34*, 3458.
- [27] Q. Wang, Q. Yan, P. F. Nealey, J. J. de Pablo, *J. Chem. Phys.* **2000**, *112*, 450.
- [28] U. Jeong, D. Y. Ryu, D. H. Kho, D. H. Lee, J. K. Kim, T. P. Russell, *Macromolecules* **2003**, *36*, 3626.
- [29] K. I. Winey, E. L. Thomas, L. J. Fetters, *Macromolecules* **1991**, *24*, 6182.
- [30] A. M. Mayes, T. P. Russell, S. K. Satija, C. F. Majkrzak, *Macromolecules* **1992**, *25*, 6523.
- [31] Q. Wang, P. F. Nealey, J. J. de Pablo, *J. Chem. Phys.* **2003**, *118*, 11278.
- [32] U. Jeong, H.-C. Kim, R. L. Rodriguez, I. Tsai, C. M. Stafford, J. K. Kim, C. J. Hawker, T. P. Russell, *Adv. Mater.* **2002**, *14*, 274.
- [33] U. Jeong, D. Y. Ryu, J. K. Kim, D. H. Kim, T. P. Russell, C. J. Hawker, *Adv. Mater.* **2003**, *15*, 1247.
- [34] U. Jeong, D. Y. Ryu, J. K. Kim, D. H. Kim, X. Wu, T. P. Russell, *Macromolecules* **2003**, *36*, 10126.
- [35] J. L. Wang, T. Grimaud, K. Matyjaszewski, *Macromolecules* **1997**, *30*, 6507.
- [36] K. Matyjaszewski, J. L. Wang, T. Grimaud, D. A. Shipp, *Macromolecules* **1998**, *31*, 1527.
- [37] J. Bolze, J. Kim, J. Huang, S. Rah, H. S. Youn, B. Lee, T. J. Shin, M. Ree, *Macromol. Res.* **2002**, *10*, 2.